Development of a CubeSat Propulsion System

IEPC-2025-705

Presented at the 39th International Electric Propulsion Conference
Imperial College London • London, United Kingdom
14-19 September 2025

Stephen Clark[1], Francesco Guarducci[2], Dominic Marangone[3], Rhodri Lewis[4], Alexander J.N. Daykin-Iliopoulos[5], Klevis Gasa[6] Graham Skingle[7] and Peter Turner[8]
Mars Space Ltd, Southampton, United Kingdom

Maria Smirnova[9] and Aloha Mingo[10]
TransMIT GmbH, Giessen, Germany

Phil McNutt[11]
TWI Ltd, Granta Park, Great Abbington, Cambridge, CB21 6AL, UK

Joseph Kigonya[12]
Techline Systems Limited, 20A Picton House, Waterlooville, Hampshire, PO7 7SQ, UK

Johan Kuiper[13]
Bradford Space, De Wijper 26, 4726 TG, Heerle, The Netherlands

Emilia Wegrzyn[14]
AVS UK Ltd, URA Building 9002, Westcott Venture Park, Aylesbury, HP18 0XB, UK

Neil Wallace[15]
European Space Agency, Noordwijk, The Netherlands

[1] Head of AIT, Mars Space Ltd, stephen.clark@mars-space.co.uk
[2] Director, Mars Space Ltd, francesco.guarducci@mars-space.co.uk
[3] Electric Propulsion Engineer, Mars Space Ltd, dominic.marangone@mars-space.co.uk
[4] Senior Electric Propulsion Engineer, Mars Space Ltd, rhodri.lewis@mars-space.co.uk
[5] Senior Research Engineer, Mars Space Ltd, alexander.daykin@mars-space.co.uk
[6] PhD Candidate, Faculty of Engineering and Physical Sciences, kg2n21@soton.ac.uk
[7] Senior Mechanical Engineer, Mars Space Ltd, graham.skingle@mars-space.co.uk
[8] Propulsion Systems Engineer, Mars Space Ltd, peter.turner@mars-space.co.uk
[9] Project division director, IQM, maria.smirnova@transmit.de
[10] Lead Electric Propulsion Engineer TransMIT IQM Project division, aloha.mingo@transmit.de
[11] Principal Engineer, Surfacing, Corrosion and Interfaces department, TWI Ltd, phil.mcnutt@twi.co.uk
[12] Technical Director, Techline Systems Limited, j.kigonya@techline-systems.co.uk
[13] System Engineer, Bradford Space, j.kuiper@bradford-space.com
[14] Senior Mechanisms Engineer, AVS UK Ltd, ewegrzyn@a-v-s.uk
[15] Senior Electric Propulsion Engineer, TEC-M, Neil.Wallace@esa.int

Abstract: The use of high specific impulse (SI), high total impulse (Ns) electric propulsion technology is rapidly gaining traction and will significantly enhance the performance capabilities of small spacecraft (including CubeSats). Performance improvements will enable commercial applications and scientific missions previously inconceivable with this class (and cost) of spacecraft. Example applications are Low Earth Orbit (LEO) mega constellations, Space Weather Study, Ultra-Low Earth Orbit observation and GPS/Comms. The target 12U CubeSat can achieve significant scientific return at dramatically lower cost of larger missions when equipped with a Miniaturised Electric Propulsion System with the following characteristics, Single Thruster plus Neutraliser function, total impulse >75kNs, specific impulse >3200s and thrust range from 0.8mN to 2.2mN at powers <120W.

Nomenclature

AIT	=	Assembly Integration and Test
CEPS	=	CubeSat Electric Propulsion System
CGT	=	Cold Gas Thruster
CPS	=	CubeSat Propulsion System
DN	=	Dry Neutraliser
EM	=	Engineering Model
EP	=	Electric Propulsion
EPL	=	Electric Propulsion Laboratory
FMS	=	Fluid Management System
FCV	=	Flow Control Valve
FDIR	=	Failure, Detection, Isolation and Recovery
FDV	=	Fill and Drain Valve
HP	=	High Pressure
HPF	=	High Pressure Filter
HPIV	=	High Pressure Isolation Valve
HPT	=	High Pressure Transducer
LEO	=	Low Earth Orbit
LP	=	Low Power
LPT	=	Low Pressure Transducer
MRCS	=	Miniature Reaction Control System
NCS	=	Neutraliser Casing Supply
NGT	=	Neutraliser Gate Supply
NHV	=	Negative High Voltage
OBC	=	On-Board Computer
PGS	=	Plasma Generator Supply
PHV	=	Positive High Voltage
PPU	=	Power Processing Unit
PSMS	=	Propellant Storage and Management System
QM	=	Qualification Model
RFG	=	Radio Frequency Generator
RIT	=	Radio-Frequency Ion Thruster
TPM	=	Thruster Pointing Mechanism
TPME	=	Thruster Pointing Mechanism Electronics
TRL	=	Technology Readiness Level
ULEO	=	ultra-Low Earth Orbit
W	=	Watts
Xe	=	Xenon

I.Introduction

Mars Space are responsible for the development of the full CubeSat Propulsion System (CPS) architecture, which consists of the CubeSat Electric Propulsion System (CEPS) and the Miniature Reaction Control System (MRCS). For CEPS, Mars Space are currently developing a miniaturised ion thruster (RIT3.5) along with a Dry Neutraliser Technology (DN3.4) [8] whilst the MRCS utilises cold gas thrusters (CGTs). Mars Space will also lead the interface definition, management and testing of the other sub-systems comprising of the pointing mechanism, miniaturised flow control system, propellant storage tanks and PPU.

Mars Space activities include the specification for a 12U CubeSat application in conjunction with the agency for the overall System Engineering tailored to ECSS specifications for CubeSat. Elements of the sub-system will be coupled together with the overall objective of demonstrating the system performance capability.

This paper presents the design, development, and testing of a miniaturised Electric Propulsion System specifically tailored for CubeSat applications. CubeSats, with their small form factor, are increasingly used for various space missions, and efficient propulsion systems are crucial for orbital manoeuvres and extended mission lifetimes. The proposed electric propulsion architecture offers a compact and low-power solution.

The system aims to enhance CubeSat capability/manoeuvrability. Simulations and modelling are being used to optimize the thruster's performance for CubeSat missions. The project involves a series of ground tests to validate the functionality, efficiency and thrust characteristics. Preliminary results demonstrate promising performance metrics, including specific impulse and thrust-to-power ratio, highlighting the potential viability of the system for CubeSat applications. The development status of each individual critical subsystem will be summarised along with the results of the ongoing coupling tests. The firing of the RIT3.5 and DN3.4 at the EPL facility in ESTEC is shown in Figure 1. The AIT strategy at both system and spacecraft level will also be detailed.

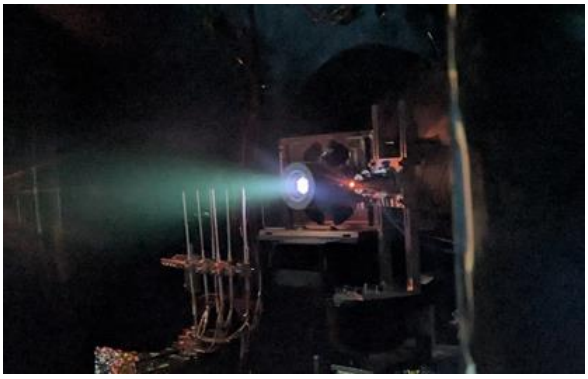

Figure 1. MSL EM-RIT3.5 in operation coupled with the MSL EM-DN3.4

Furthermore, the paper discusses coupling tests and architecture considerations for CubeSats, addressing challenges related to mass, power constraints, and thermal management. In particular, the CPS architecture that Mars Space Ltd has specifically tailored for the HENON mission [2] is also outlined, providing an overview of the solutions implemented to integrate the different subsystems. The scalability and adaptability of the proposed system make it suitable for a wide range of CubeSat missions, from Earth observation to deep space exploration.

II. Cubesat Propulsion System Architecture

The MSL Electric PROpulsion Platform, "EPROP", module architecture for CubeSats and small spacecraft is shown in Figure 2. The compact propulsion system delivers high specific impulse (>3,000 s), total impulse (>75 kNs), and a variable thrust range of 0.8–2.2 mN at low power consumption (<120 W). EPROP represents a step-change in propulsion for small spacecraft, enabling extended operational lifetimes, complex orbital manoeuvres, and access to new mission profiles beyond current capabilities.

This targeted development programme culminates in a flight demonstration by December 2026 to enable the Heliospheric Pioneer for Solar and Interplanetary Threats Defence (HENON) Mission.

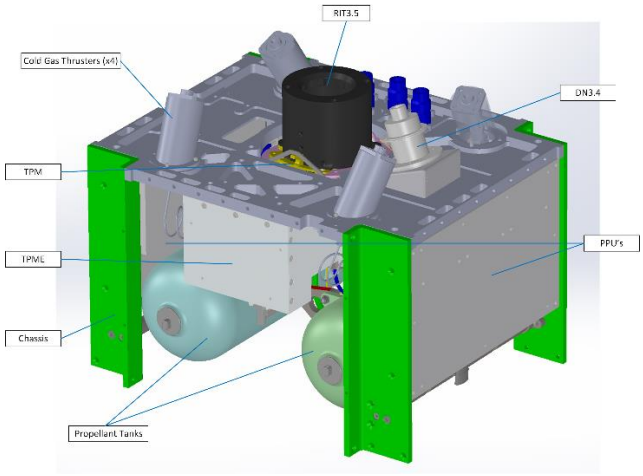

Figure 2. EPROP Module Architecture

The EPROP module is a very compact module, with dimensions H=190mm, W=250mm and L=300mm. This fully integrated, plug-and-play electric propulsion (EP) platform offers a scalable, off-the-shelf solution for both commercial and public-sector customers deploying constellations. As such, this project aims to establish a UK-led, globally competitive capability in enabling affordable, high-performance spacecraft operations whilst unlocking significant scientific and commercial returns at a fraction of the cost of traditional large-scale missions. Target applications include: (1) deployment of large-scale constellations in Low Earth Orbit (LEO), (2) space weather monitoring and heliophysics missions, (3) sustained operations in ultra-Low Earth Orbits (ULEO) via drag compensation, (4) Lunar/Martian navigation and communication constellations, and (5) deep-space exploration such as planetary flybys and asteroid missions.

The CPS consists of the following components, which are summarized in this paper:

1) RIT3.5
2) Dry Neutraliser (DN3.4)
3) PPU's (A+B) with integrated RFG
4) Propellant Tanks (x2)
5) Flow Management System (FMS)
6) Propellant Storage and Management System (PSMS)
7) Thruster Pointing Mechanism (TPM)/Thruster Pointing Mechanism Electronics (TMPE)
8) Cold Gas Thrusters (CGT x4)

As detailed above and in Table 1, the CPS has a throttleable EP System and thrust vector pointing mechanism that optimises performance, lifetime and propellant utilisation, negating the need to frequently offload torque from conventional 'static' EP systems.

Table 1. CubeSat Propulsion System Performance Targets

Total impulse	>75kNs
Specific Impulse	>3200s
Throttle Range	0.8mN to 2.2mN
Power Range	<120W

The mode transition diagram shown in Figure 3, defines the discrete operational modes of the CEPS system. The architecture is designed to only require high-level commands from the spacecraft, while the propulsion unit autonomously executes the detailed sequencing.

The mode diagram highlights the key operational states such as STANDBY, STARTUP, DISCHARGE and THRUST. With built in Failure, Detection, Identification and Recovery (FDIR), autonomous protection and reporting can be achieved and communicated with the spacecraft allowing the system to transition to safe modes in the event of an anomaly. By encapsulating the main control logic inside of the EP system, the spacecraft is only required to provide simple, high-level commanding, reducing operational overhead and interface complexity.

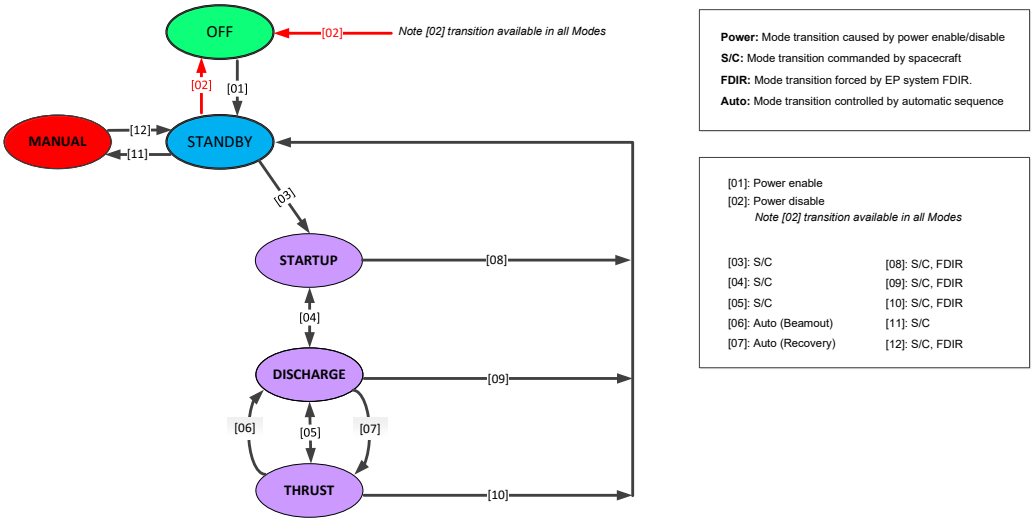

Figure 3. CEPS EP Mode Transition Diagram

The CPS (CEPS + MRCS) dry mass target is ≤6.5kg, including maturity margins.

III.RIT3.5

The MSL-RIT3.5 radiofrequency ion thruster was originally designed and developed in the frame of ESA technology development projects targeting applications such as the Next Generation Gravity Mission (NGGM). The RIT3.5 has recently been the subject of a collaboration agreement through which Mars Space Ltd (MSL) has acquired the design rights from TransMIT GmbH. MSL (with support from TransMIT) is industrialising the design, establishing an industrial manufacturing supply chain and advancing the technology for precision control satellite applications such as NGGM, as well as for deep space CubeSat class missions such as HENON [2].

The RIT3.5 is a miniature radiofrequency gridded ion thruster capable of generating thrust in the range 50 μN to 2.5 mN (in a 2-grid or 3-grid configuration). The thruster is comprised of the following main functional elements:

- **Ionizer**: Consisting of a ceramic discharge chamber and RF coil for generating an inductive plasma discharge.
- **Gas Supply**: Comprising the propellant gas feedline to the discharge chamber, which incorporates a gas isolator. The gas isolator provides electrical isolation between the high voltage potential (being the plasma potential which floats just above the positive high voltage (PHV) potential of the screen grid) within the discharge chamber and the gas feedline connected to S/C ground.
- **Grid System**: Consisting of a two or three grid extraction system and a ceramic grid support and alignment structure. Each of the three grids is electrically isolated from the thruster casing and from each other. The grids are normally referred to as the "Screen", "Accel" and (where fitted) "Decel" grids, ordered in the direction of ion beam extraction.
- **Thruster Housing and Interface**: Consisting of thruster casing and support structures, a thruster back plate with interface connections for HV, RF and propellant to the thruster assembly, and fixings for the HV lines, RF coil and gas inlet.

When MSL acquired the design rights to the RIT3.5 thruster from TransMIT GmbH it had already benefitted from many years of development, with activities targeting both precision control applications and CubeSat applications. Work undertaken by MSL has focused on adapting the existing design in response to the latest requirements, and industrialization of the design to meet the needs of a flight mission, whilst preserving critical elements of the functional design such as the discharge chamber and RF coil geometries, gas distribution system and general grid configuration, in order to retain valuable development heritage.

Figure 4. MSL's RIT3.5 Engineering Model.

MSL completely redesigned the rear interfaces of the thruster, replacing bulky electrical and fluidic connectors with flying lead arrangements configured for simplest possible system integration. The MSL designs benefit from prior experience of larger thruster developments, in order to achieve robust designs with respect to mechanical clamping for strain relief, electrical bonding of cable shields and electrical shielding. Other industrialization activities included: establishment of a complete set of detailed RIT3.5 technical specifications and drawings; development of a new (primarily UK-based) supply chain drawing from MSL's experience on other developments; and implementation of a full in-house production capability based at MSL's Adanac site in Southampton, UK.

The design of the ion optics, specifically the grid assembly, is a key factor in the performance and lifetime of any gridded ion thruster. For MSL's propulsion system development intended for CubeSat missions such as HENON, the RIT3.5 thruster has been tailored to support steady-state operation at a limited number of thrust setpoints, consistent with typical small satellite propulsion requirements. A two-grid configuration has been baselined for the CubeSat system, consisting of a positively biased screen grid and a negatively biased accelerator grid. This configuration is optimal for compact platforms where simplicity, efficiency, and flight heritage are priorities. The selected grid geometry and operating parameters were optimised to support reliable performance across the anticipated mission profile, while minimising erosion as far as possible and therefore extending component lifetime.

The optimisation process included heritage-based modelling activities, using tools developed during previous gridded ion thruster programmes. Firstly, an ion optics performance model built on the FFX simulation code was used to establish suitable ion optics design to achieve the required beam current for the desired operating conditions, and to ensure that each grid pair was operating away from perveance limits and crossover limits as far as possible. This was conducted in conjunction with existing discharge and electrical performance models in consultation with TransMIT GmbH. The FFX code was then used to perform a grid erosion assessment representing steady-state thrust operation, and confirm that the predicted grid lifetime met the anticipated mission requirement. This included predictions of the electron back-streaming margin as a function of cumulative operating time. This analysis identified the ion optics design parameters to be adopted in the grid design, and confirmed that the thruster is expected to meet the lifetime requirement with margin.

Note that the RIT3.5 mechanical design allows for integration of an optional third grid, known as the decelerator (or decel) grid. The three grid electrode plates are all electrically isolated from each other and from the thruster casing, allowing the thruster to operate in either two or three grid configurations without mechanical modification. In the two-grid configuration, the front grid plate is replaced by an isolated electrode ring. This approach ensures the thruster can be adapted for other mission types without requalification of the mechanical configuration. The three-grid configuration has been adopted for the NGGM precision control application [9]. The three-grid configuration can also be readily adapted to achieve the novel variable Isp performance previously demonstrated by TransMIT GmbH [10].

The final baseline RIT3.5 configuration for MSL's CubeSat propulsion system provides a balance between simplicity, lifetime, and performance, whilst the thruster design benefits from the modular ion optics design that supports future mission reuse.

IV.Dry Neutraliser (DN3.4)

The DN3.4 dry neutralizer is a recent development by MSL, designed to provide neutralizing current for electric micro-propulsion systems operating in the micro-Newton to milli-Newton thrust range, with a capability of supporting up to 2.5 mN. This makes it well suited for CubeSat-class missions such as HENON, which demand compact, efficient, and fully integrated propulsion subsystems.

Unlike conventional hollow cathode technologies, the DN3.4 does not require propellant for operation. This "dry" approach eliminates the need for a fluidic supply system, thereby simplifying the overall propulsion architecture and improving system reliability for small satellite platforms. Additionally, the absence of neutralizer propellant removes any potential impact on system-specific impulse, enabling more accurate mission-level performance predictions.

For the HENON mission, the DN3.4 has been selected as the baseline neutralization technology. Its compact form factor and lack of consumables make it particularly attractive for volume- and mass-constrained CubeSat missions.

The DN3.4 is composed of three main functional subsystems:

- **Emitter:** The emitter consists of a barium oxide emitting surface with a potted heating element and housed within a refractory metal frame. A dedicated heatshield encloses the emitter to minimise radiative thermal losses, thereby improving heating efficiency and operational stability.
- **Electrode System:** The extraction system comprises three electrodes: a focusing electrode, gate electrode and casing electrode. The focusing electrode is electrically bonded to the emitter, and all three electrodes are electrically isolated from each other, with the casing electrode forming the neutralizer
- **Housing:** This tri-electrode configuration facilitates efficient extraction and shaping of the electron plume.
- **Neutralizer Housing and Interface:** The housing supports the internal components and provides mechanical and electrical interfaces. Flying leads connect to the heater and electrodes, allowing independent control of

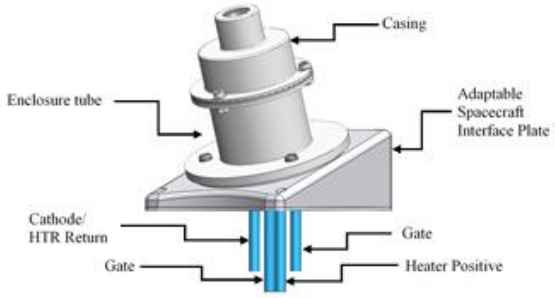

Figure 5. QM-DN3.4 CAD Model

each function. The housing also serves as the structural interface to the wider propulsion system and spacecraft.

The DN3.4 is currently undergoing performance and lifetime testing in support of the HENON mission.

Initial test results indicate stable electron emission and a controllable beam profile. With demonstration of coupled operation with the RIT3.5 thruster under mission-representative conditions presented in this paper. The modular nature of the DN3.4 design supports scalability and integration with a range of micro-propulsion platforms beyond HENON.

To accelerate the maturation of this technology, a structured development programme was undertaken. The first phase involved a core technology trade-off and down-selection process, including material sample testing and analysis in collaboration with academic partners. Based on these outcomes, a Breadboard Model (BBM-DN3.4) was developed, incorporating initial electrostatic modelling.

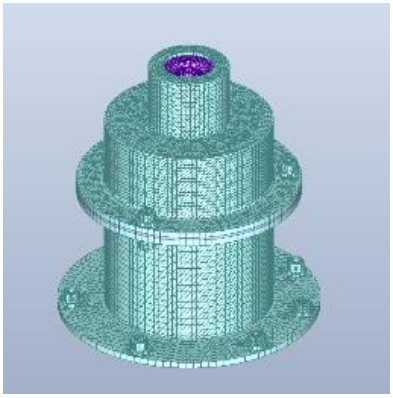

Figure 6. EQM-DN3.4 CAD

V.Propellant Tanks

This section of the paper provides an overview on the development of the propellant tanks that TWI are responsible for. TWI have been working closely with MSL and ESA to develop the propellant tank specification. TWI have produced a detailed tank design, including finite element modelling, and are heavily in the process development work to realise its manufacture to the standards specified in the specification and CubeSat ECCS guidelines.

TWI will manufacture and destructively test propellant tanks as per the developed processes and validate/refine the tank design, if required. TWI will then produce propellant tanks using this developed process, which shall undergo a battery of tests, as per ESA design validation guidelines.

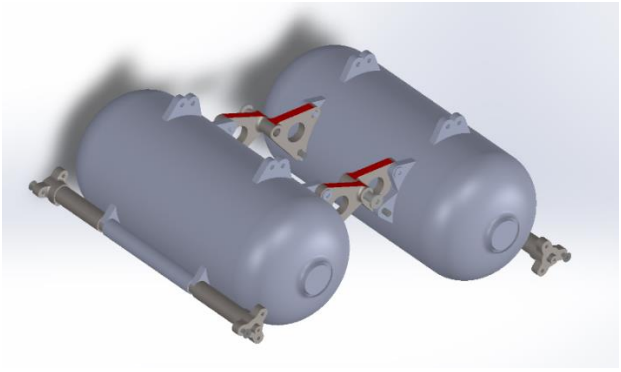

Figure 7. CAD Layout of EPROP Twin Propellant Tanks Architecture (Showing support RODS and Inter-tank bracketry)

B. Cold Spray Additive Manufacturing

Cold spray is a solid-state coating and additive manufacturing process in which fine metal powders are accelerated to supersonic velocities using a high-pressure gas stream. The particles are directed onto a substrate where their extremely high kinetic energy causes severe plastic deformation and bonding, without melting.

Because deposition occurs below the melting temperature, cold spray avoids issues common to conventional thermal spray processes, such as oxidation, phase transformations, and residual thermal stresses. As a result, the process produces dense, oxidation-free deposits with properties close to bulk material. This makes cold spray attractive for applications such as repairing high-value components, fabricating large or complex structures, and processing temperature-sensitive alloys like titanium and aluminum.

Although cold spray can be used for additive manufacturing via layer-wise deposition, the process has limitations. The relatively wide jet, turbulence at the substrate/deposit interface, and its line-of-sight nature restrict the ability to achieve fine features or intricate geometries. Consequently, deposits are near-net shape but typically require post-processing or alternative strategies to achieve the desired component fidelity.

To overcome these limitations, an alternative approach was developed by TWI. Instead of free-form deposition, a thin cold spray layer was applied to the external surface of a sacrificial mandrel, which was pre-machined to replicate

the internal geometry of the final part. After deposition, the mandrel was removed, leaving a seamless thin-walled component.

While the as-deposited structure has some "green" strength, it requires heat treatment to achieve the final mechanical properties. Heat treatment promotes diffusion bonding between particles and the development of a refined microstructure suitable for end-use applications.

During optimisation of this process, several challenges were identified:

- Cold spray parameter optimisation – tuning gas pressure, temperature, powder feed rate, and standoff distance for dense, defect-free deposits.
- Sacrificial mandrel manufacture and processing – ensuring accurate geometry, controlled surface finish, and reliable removal.
- Toolpath optimisation for robotic deposition – developing strategies to achieve uniform layer thickness and consistent coverage.
- Heat treatment development – identifying conditions that promote particle bonding and microstructural evolution to achieve required mechanical properties.

C. Cold Spray Parameter Development

Parameter development trials were undertaken to establish the optimal conditions for cold spray deposition. Critical process variables such as gas pressure and gas temperature were systematically varied, with their influence on deposit density and microstructure evaluated.

During these trials, it was determined that the quality of the powder feedstock was of critical importance. Particle size distribution, morphology, and chemical composition all had a pronounced effect on deposit density and quality.

D. Sacrificial Mandrel Development

Initial work employed aluminium mandrels, which were removed post-deposition through dissolution in sodium hydroxide. This approach was constrained by the slow dissolution rate, often requiring several days and generating large volumes of hazardous waste. To reduce dissolution times, hollow aluminium mandrels were fabricated; however, this introduced additional cost and delays, as the process required CNC machining of hollow sections, followed by welding and final machining to tolerance.

To address these limitations, TWI developed a novel re-usable mandrel system that enables rapid removal and recycling of the mandrel material, while eliminating the generation of hazardous waste.

E. Toolpath Optimisation

The additive manufacturing process required continuous mandrel rotation while the spray gun traversed across its surface. To maintain constant peripheral speed and consistent track spacing over varying diameters, the mandrel's rotational speed had to be dynamically adjusted.

Un-optimised toolpath may contribute to increased porosity in critical areas. A robot-integrated servo-motor driven lathe was therefore designed and built, allowing precise toolpath control via offline programming. This system also enabled the deposition of integrated structural features onto the propellant tank body, eliminating the need for separate brackets. Such integral features reduced mass and simplified the assembly of CubeSat hardware.

F. Heat Treatment Development

Vacuum heat treatment trials were performed to balance strength and toughness in the deposited Ti-6Al-4V material. While Hot Isostatic Pressing (HIP) is commonly recommended for consolidating additively manufactured parts, it was found to be less effective in this case, likely due to the thin wall sections and the presence of inter-particle boundaries that act as diffusion pathways for the process gas, limiting the effectiveness of the HIP process for thin sections.

Heat treatment was found to be most effective using a vacuum heat treatment approach, consisting of solution treatment and ageing, with the solution temperature kept below the beta transus. This retained a fine equiaxed microstructure, as the alpha phase acted to pin grain boundaries and suppress grain growth, thereby maintaining high strength without significant loss of toughness.

VI.Power Processing Unit (PPU)

The Power Processing Unit (PPU) for the EPROP module has been developed in the UK by Techline Systems.

The initial stages of the PPU development focused on the following key elements:

- PPU requirements capture
- PPU electrical architecture (see Figure 8)
- PPU mechanical design concept
- Detailed design of the critical circuit elements namely the high-voltage and high-frequency power supplies
- PPU Preliminary Mechanical Design

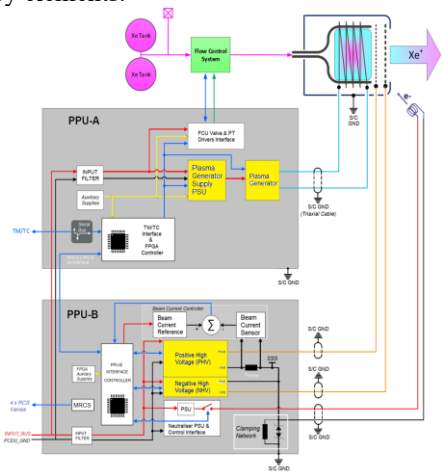

Figure 8. EPROP PPU Architecture

Detailed design of the critical elements of the PPU have been addressed during a de-risk activity. The critical elements are highlighted in YELLOW in Figure 8 and are as follows:

- Positive High Voltage (PHV) supply design
- Negative High Voltage (NHV) supply design
- Plasma Generator Supply (PGS) Design (shown in Figure 10) - PGS Output Stage design and PGS Power Supply
- PPU Grounding Scheme

Due to the different functional power supplies accommodated in each PPU (PPU & PPUB), the dimensions are marginally different and have the following properties:

PPU-A: L=200mm, W=129mm, H=48mm

PPU-B: L=205mm, W=129mm, H=69mm (inc HV terminal blocks)

The PPU is configured with 2 x 28V bus inputs, each dedicated for the EP system and Micro Reaction Control System (MRCS) Module. Equally a dedicated OBC CAN interface is provided for the EP System and a RS422 communications interface for the MRCS module – see Figure 9. Simultaneous operation of the EP system and the MRCS system is not envisaged during nominal operations. Furthermore, their respective power and communication interfaces are fully independent to eliminate potential cross-coupling or resource contention. The PPU incorporates autonomous sequencing, continuous surveillance, and Fault Detection, Isolation and Recovery (FDIR) features, ensuring safe and reliable operation with minimal reliance on spacecraft commanding. As a result, spacecraft interaction is limited primarily to the provision of housekeeping telemetry and the execution of top-level control commands.

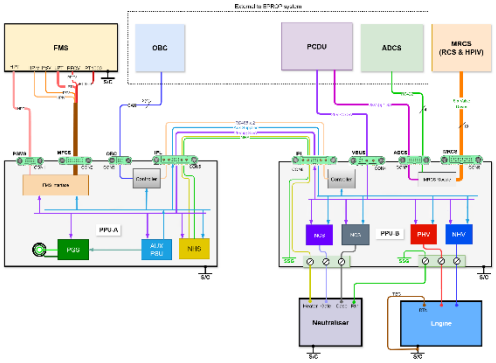

Figure 9. PPU Power/Comms Architecture

Conclusion of this activity establishes credible baseline designs to facilitate rapid development of a fully integrated PPU compatible with a 12U CubeSat format based on the RIT3.5 thruster. Following the first flight opportunity, the plan is to market the PPU as part of a fully integrated EPROP system for commercial or science-based deep space CubeSat applications.

The PPU specification has been tailored to meet the general requirements for the HENON mission - an ESA Interplanetary CubeSat To Monitor Space Weather Phenomena. The critical elements of the PPU have been designed, manufactured, and successfully bench tested using thruster load simulators and preliminary coupling tests (see Section XI). Several evaluation coupling tests have been successfully completed at the ESTEC EPL facility to establish compatibility with the target RIT3.5 RF thruster. The coupling test is considered a significant achievement since it validates the baseline designs with a representative thruster/plasma load. The Dry Neutraliser power supply specification, design and preliminary coupling tests have also been successfully completed during the coupling test.

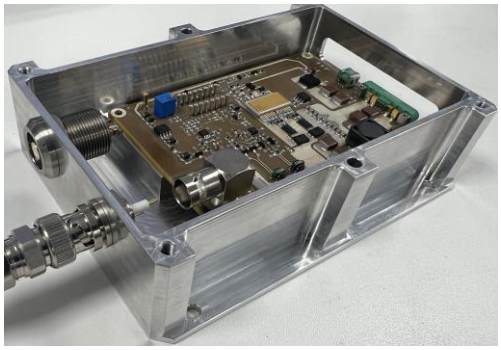

Figure 10. Prototype Plasma Generator Power Supply (PGS) De-risk Hardware

The de-risk and coupling test activity have allowed rapid development of key elements of the PPU which includes upfront identification or elimination of design issues or potential problem areas. This allows upfront strategic planning and resourcing including make/buy trade-offs based on schedule and experience. The de-risk PPU hardware has been proven with a flight representative thruster. This key milestone now facilitates rapid development of a fully integrated PPU.

A follow-on activity for the PPU is currently live and fully funded by ESA to migrate the de-risk hardware to a fully integrated EM PPU followed by a fully qualified FM PPU. Target TRL is 8. Flight qualification is expected by Q2, 2026. Target mission: HENON pathfinder mission. (HEliospheric pioNeer for sOlar and interplanetary threats defeNce). Mission type: Science, Sun-Earth Space Weather observations / predictions. Planned launch date: December 2026.

VII.Flow Management System (FMS)

Bradford Space have been developing an electric propulsion flow/pressure control solution that eliminates a large number of high-pressure components that are typically seen in Electric Propulsion systems (i.e. latch valve, mechanical pressure regulator etc.). This approach has a few significant benefits over traditional EP architectures, most notably the reduction of cost, reduction of complexity, the reducing of mass/size and an overall simplification of the functional architecture. With the removal of these high-pressure components, more emphasis is devoted to the Flow Control Units, which are typically low-pressure flow controllers, dedicated to a specific EP thruster. This emphasis for high pressure operation of the typical Flow Control Units is the goal of the development of the LP FMS.

A. Low Power Fluid Management System

The functional schematic of the LP FMS architecture is presented in the Figure 11:

The LP FMS requires some common upstream elements (all of which are incorporated in the PSMS architecture of the CPS system- see section IX):

- FDV, Fill & Drain Valve, for propellant loading/unloading, as this does not rely on the amount of EP thrusters. In addition, the location of the FDV on the spacecraft must be such that external access is possible. Also, thermal control of the high-pressure tubing in the common section has to be guaranteed, even with the LP FMS switched off, hence is typically performed by the spacecraft thermal control system;
- HPT, High pressure Transducer, to monitor and measure the tank pressure to estimate the remaining propellant load;
- HPF, High Pressure Filter, to provide propellant filtration enabling long LP FMS operation and life;
- Tank, which is considered customer responsibility.

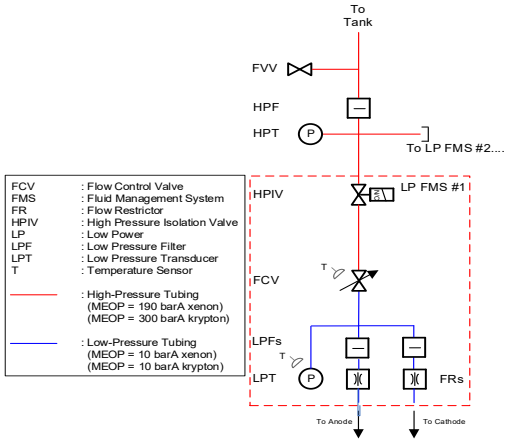

Figure 11: LP FMS Architecture

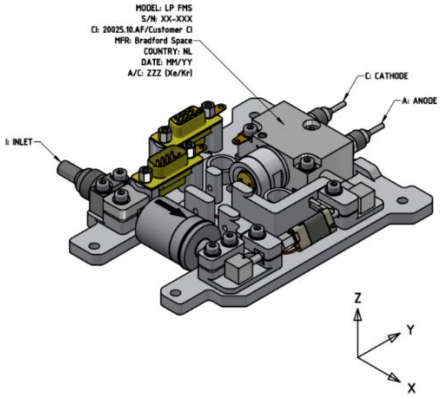

Figure 12: LP FMS Isometric View

Downstream of the common element, each EP thruster requires the use of one LP FMS, which performs pressure reduction and flow control in a single step. Implementing multiple EP thrusters simply means duplicating the LP FMS units accordingly. This results in a modular design approach and makes the design of the LP FMS flexible and largely independent of the spacecraft.

The LP FMS exhibits the following top-level features (see also table below):

- Small mass and small size;
- The design features 2 high pressure internal leakage barriers;
- The internal LPT allows for closed loop operation of the FCV;
- The flow restrictors and LPT are mounted in a single block. The temperature reading from the LPT is used to estimate the flow restrictor temperature and together with the LPT pressure reading it is possible to estimate the anode and cathode flow rates;
- 2 separate electrical connectors, one for power and one for signals.

The LP FMS is composed of the following items:

- HPIV: High Pressure Isolation Valve: normally closed high pressure isolation barrier. It has an integrated filter;
- FCV: Flow Control Valve: normally closed flow control valve for pressure/flow regulation. Can be run in closed loop by using the LPT measurement or by using the discharge current from the EP thruster. Doubles as high-pressure isolation barrier. Due to the low flow rate, the enthalpy change due to the expansion of xenon will be small (<~0.4W at 186 bar and <6 mg/s xenon, and even lower for krypton) and is fully compensated by the power dissipation of the FCV;
- LPT: Low Pressure Transducer: to measure the regulated pressure from the FCV and to identify any potential (fast) pressure built-up in the system during periods of non-firing. Full Scale (FS) measuring range from 0 barA to 10 barA. Next to pressure, also flow restrictor temperature is measured;
- FRs: Flow Restrictors: a predefined hydraulic resistance to enable the correct flow rate to the anode and cathode lines;
- T: Temperature Sensors: used to estimate the flow restrictor anode-to-cathode ratio (by integrated temperature sensor inside the LPT) and FCV temperature.

The LP FMS performance is illustrated in [7]. In summary, the LP FMS has been tested for inlet pressures between 5 bar up to 190 bar, TRP temperatures from -15^{0}C to +70^{0}C and at flow rates of 0.7 mg/s to 5.0 mg/s xenon (0.5 mg/s to 3.8 mg/s krypton). Different flow ranges and Anode-to-Cathode (A/C) ratios can be set by changing the sizing of the flow restrictors. The pressure & flow control stability can be seen to be excellent. A single PID closed loop controller setting is used for operation of the abovementioned pressure and temperature boundary conditions. In addition, the LP FMS closed loop operation is also independent of the downstream volume (i.e. tubing length) between the LP FMS and the EP thruster. Any changes to the LP FMS setpoints will only have a time delay when arriving at the EP thruster but will not generate any instabilities.

Table 2. LP FMS Performance Characteristics

Characteristic	Value
Design Life	15 years
Mass	< 400 gr
Envelope	118 x 143 x 27 mm
Inlet Tube	1/4" OD tube, suitable for orbital welding. Alternatively AS4395 connection available
Outlet Tubes	2x 2 mm OD tubes, suitable for orbital welding. Alternatively AS4395 connection available
Performance Curves	See figures 3, 4 and 5. Typical figures. Total flow rate and anode-to-cathode ratios are customizable.
Compatible Media	GN2, Xe, Kr, GHe, Ar Grade 5.0 typical.
Power budget	<3 W nominal, <11 W peak
Internal Leakage	<1E-5 scc/s GHe over pressure & non-operational temperature range.
External Leakage	<1E-6 scc/s GHe over pressure & non-operational temperature range. Fully welded
Operating Pressure Range	5-190 barA (Xe) / 5-300 (Kr)
Maximum Expected Operating Pressure	190 barA (Xe) / 300 barA (Kr)
Proof Pressure	285 barA (Xe) / 450 barA (Kr), with FCV unpowered and closed. HPIV open and/or closed
Burst Pressure	>400 barA (Xe) / 750 barA (Kr), burst qualification test to be performed to cover 400-750 bar range
Sine Vibration	5-23 Hz: +/-10 mm 23-100 Hz: 20 g Qualification completed.
Random Vibration	20.5 Grms (In-Plane) 23.04 Grms (Out-Of-Plane) Qualification completed.
Shock	100 Hz: 20 g 1000 Hz: 2000 g 10000 Hz: 2000 g Qualification completed. One shock per axis.
Operating Temperature Range	-20^{0}C to +75^{0}C Qualification range.
Non-Operating Temperature Range	-20^{0}C to +75^{0}C Qualification range.

At the heart of the LP FMS, which is key in its performance, is the flow control valve. The flow control valve is a thermally controlled proportional regulation valve. This flow control valve has been named as a game changer in proportional flow control due to a variety of reasons:

- The fluidic elements from the flow control valve are made up of only 5 unique mechanical parts, which are an example of its simplicity;
- These 5 mechanical parts are assembled manually, without the need for any specialized tooling;
- The low part count and overall simplicity ensure a cost-effective product, with low production throughput duration and potential for high rate production;
- When assembled, the valve opening temperature can be controlled manually;
- Once the correct valve opening temperature has been set, the valve is externally welded, locking the opening temperature in place. The corresponding welds are in the low-pressure operational side of the valve and as such are not exposed to stress induced by high pressure operation and/or by stress induced by repeated operation of the valve (i.e. cycling);
- During operation with either xenon or krypton, the flow control valve is able to operate nominally and deliver the required power to the xenon or krypton to prevent the enthalpy change of the gas, ensuring nominal gas temperatures at the outlet of the flow control valve, while preventing xenon liquification in the process. As such, the heat/power is transferred to where it is required;
- Due to the slower response time nature of this thermal valve compared to traditional solenoid and/or piezo operated valves, its impact demand on the PPU requirements is smaller, with the flow control valve being able to operate in closed loop using a 12-bit driver running at 20 Hz clock frequency.

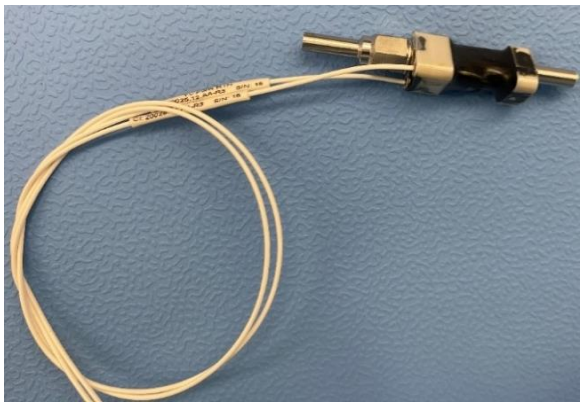

Figure 13: Flight Model Flow Control Valve

VIII.Thruster Pointing Mechanism/Electronics (TPM/TPME)

The thruster pointing mechanism (TPM) and driver electronics (TPME) for the EPROP module have been developed in the UK by AVS. This section presents the Engineering Model (EM) design of the Thruster Pointing Mechanism (TPM-250) for nanosat electric propulsion thrusters. The TPM-250 is planned to be flown in 2026 on ESA's Henon mission.

Qualification of the mechanism will take place in October this year. In particular, with Henon's TPM, the system design was challenging due to the typical nanosatellite volume, power, and mass constraints. At the same time, the requirement to fit the tubing and harness inside (particularly connectors from the thruster) limits space inside the allowable volume. Likewise, it creates the highest resistive torque contribution, which drives the whole motorisation assessment.

The EM design of the TPM-250, with designation of key components, is shown in Figure 14.

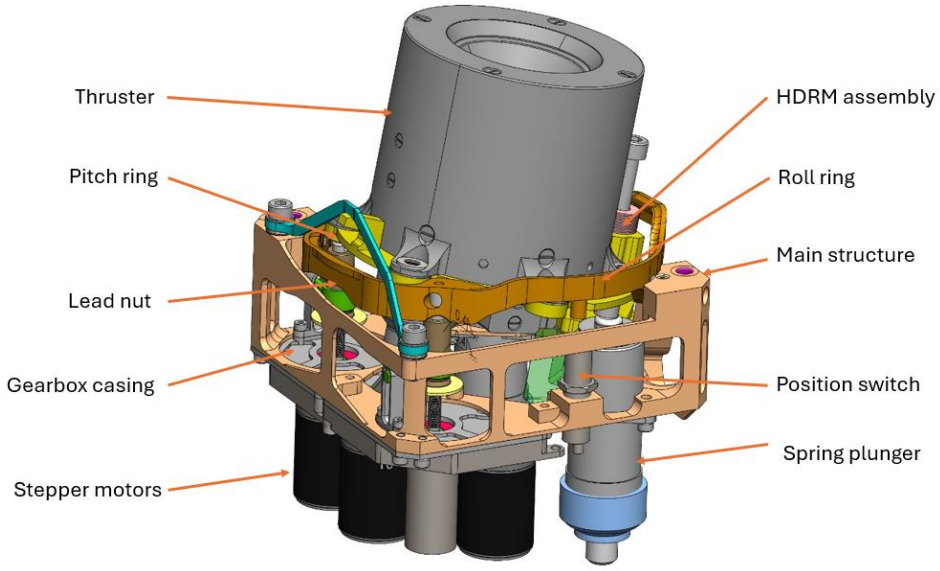

Figure 14: EM Design of the TPM-250

The TPM connects the thruster to the spacecraft structure, with the main function of orientation control. It provides a ±7.5-degree cone, with its rotation axis lateral to the flight direction. A two independent axis configuration has been implemented, where each actuation subassembly provides a rotation around one of the axes. While the actuation is fixed to the TPM structure, both axes include two supporting points via two opposed bushings. To take advantage of the space available in the corners of the assigned volume, the axes are in an "X" configuration with respect to a typical 12U CubeSat body's dimensions.

The system is controlled in an open-loop mode, and relies on high accuracy sensors to provide a homing function for the actuators. It also includes the required electric and fluidic interfaces for the thruster coming from the spacecraft. The actuation (per axis) is formed by a motor-transmission assembly and an assembly of redundant wave springs placed opposite to each other, in a perpendicular direction to the rotation axis. The primary actuation has a nut with a push contact and moving ring which rotates the platform, counteracting the spring force. An initial preload of the springs allows for the rotation in the opposite direction, so when the nut is retracted, the spring pushes back keeping constant contact with it and overcoming the resistive torques of the system. Both active actuation assemblies are in a fixed position, but the pair of springs corresponding to the thruster ring are connected to the outer ring to ensure a perpendicular contact with the first one. The system includes end-stops to limit the movement of the rings, as an added value to the functional end stops provided by the maximum compression of the spring and the maximum retraction travel of the nut. Pictures form EM testing are in Figure 15.

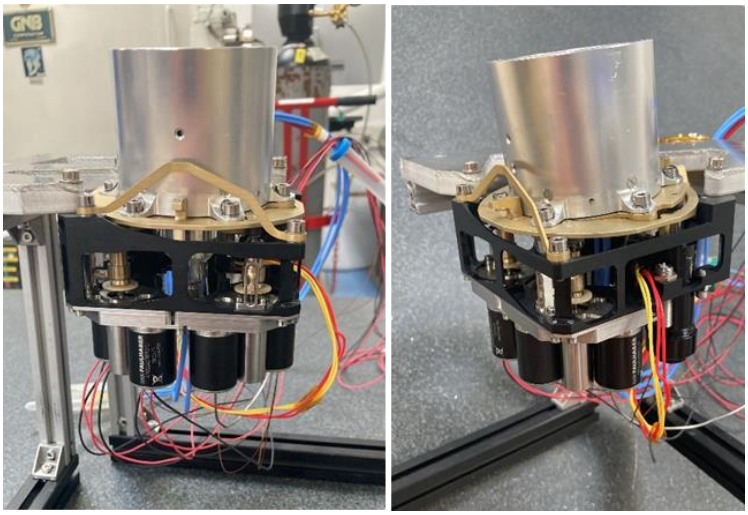

Figure 15: TPM-250 EM Testing

Coupling testing of both EM models of the TPM-250 and TPME were carried out, and in Figure 16 a picture shows the setup. The TPM performed as expected when coupled to the TPME and its measured pointing accuracy is 0.01 degree in ambient.

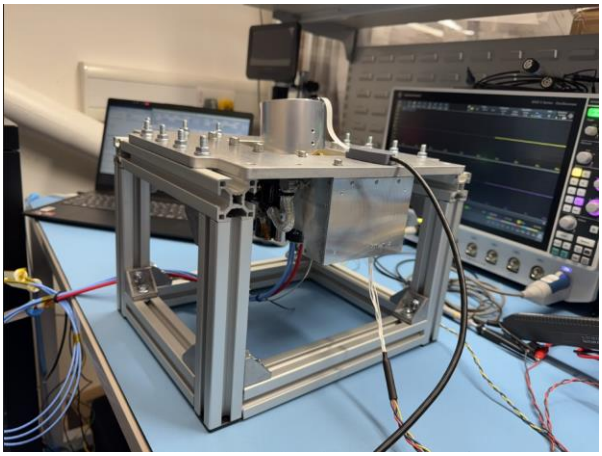

Figure 16: TPM-250 and TPME Coupling Test Setup

The main parameters of the TPM are presented in Table 3:

Table 3: TPM-250 Datasheet

TPM-250 Datasheet	
Volume	100 x 100 x 85mm
Mass	700g
Payload capabilities	500-1200g, < Ø160mm
Thruster Power	100-300W
Power (operating)	5-15 W
Power (peak)	10-20 W
Angular range	± 7.5° (2 DoF cone)
Resolution	<0.004°
Pointing accuracy	<0.08°
Rotation speed	~0.3 °/s
Number of cycles	500 (flight) + 50 (ground)
Operating temperature	-40,+70°C Thruster temp ~ <250C
Volume of electronics	100 x 71.5 x 75mm
Mass of electronics	410 g
Lifetime	>3.5 years
Applications Market Entry	Henon (2026)

IX.Propellant Storage and Management System (PSMS)

The PSMS encompasses the full fluidic network from the high-pressure propellant storage including thermal control to prevent liquification, through to the controlled delivery of propellant to each of the thrust branches (CEPS and MRCS).

The PSMS is comprised of the following equipment/sub-systems:

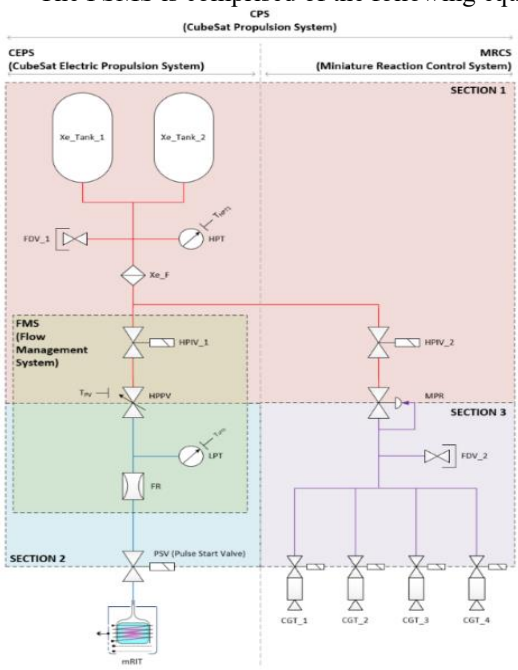

Figure 17. Propellant Storage and Management System (PSMS) Schematic

1. 2 x Xenon tanks for propellant storage, as per Section V.
2. 1 x High Pressure Transducer (HPT) for propellant gauging.
3. 1 x System Filter (Xe_F).
4. 1 x Isolation valve (HPIV_2) for MRCS isolation.
5. 1 x FMS, as per Section VII, for all-in-one pressure and flow management. Includes CEPS isolation capability.
6. 1 x Pulse Start Valve (PSV) for RIT3.5 ignition.
7. 1 x Mechanical Pressure Regulator (MPR), for MRCS pressure management.
8. 2 x Fill and Drain Valves (FDVs) to enable propellant loading and system integration / test.

The PSMS is split into three key sections:

- Section 1: High pressure section of pipework including tanks.
- Section 2: Low pressure section, flow controlled via FMS for RIT3.5 propellant feed.
- Section 3: Low pressure section, pressure controlled via MPR for CGT propellant feed.

X.Cold Gas Thruster (CGT)

The SVT01 cold gas thrusters (CGTs) for the EPROP module has been developed in the UK by Nammo. CGTs offer a simple, robust, and clean propulsion and control method, making them ideal for missions sensitive to contamination or requiring fine-grained manoeuvrability. The Nammo SVT01 thruster, a flight-proven component, provides a reliable solution for these needs, leveraging a unique design to ensure long-term, leak-free operation.

For MRCS, the SVT01 thruster uses pressurised Xenon gas, expelled through a nozzle which can be fine-tuned per customer and mission requirements without affecting qualification. The SVT01 can also operate with GN2.

Figure 18: Nammo SVT01 Cold Gas Thruster

A key feature of its design is the use of a flat-faced seal, which significantly reduces the risk of valve internal leakage over the thruster's operational lifetime, a critical factor for missions with multi-year durations. Key performance specifications include a thrust range of 10 to 200 mN and an operational pressure of 1 to 5 bar(A). The thruster has a low mass of less than 60 g and a rapid response time of under 6.0 ms, enabling precise and responsive satellite control. The body and magnetic components are constructed from Stainless Steel 304L and Radiometal 4550, with a Silicone or EPDM seal.

The SVT01 thruster's reliability is best demonstrated by its extensive flight heritage spanning more than 20 years. Its robust performance has been proven on numerous missions, including but not limited to:

- SWARM: The European Space Agency's SWARM constellation, launched in 2013, uses cold gas thrusters for drag compensation and precise orbit maintenance to measure Earth's magnetic field.
- GRACE-FO: The Gravity Recovery and Climate Experiment (GRACE Follow-On) mission, which was launched in 2018, relies on similar cold gas thrusters for maintaining the precise separation distance between its two satellites.
- Cryosat-2: The Cryosat-2 mission, launched in 2010, uses propulsion to maintain its orbit, allowing it to accurately measure changes in the thickness of polar ice sheets and floating sea ice. The successful application of the SVT01 thruster on these long-duration missions serves as a testament to its engineering quality and suitability for critical space applications.

XI.EPROP Coupling Tests

Mars Space has undertaken a series of coupling tests, initially focusing on the thruster, dry neutralizer and PPU. Naturally, the PPU design needs to be undertaken in conjunction with the thruster, as the dynamic plasma load, transients and noise propagation can only be achieved in a realistic setup (i.e. not with static resistors). The very first characterisation of the RIT3.5 for CubeSat was evaluated with EGSE/RF Grade RFG and FGSE. A hollow cathode was used as a neutralization source (HC4) and also allowed some ignition trials utilizing the electrons from the hollow cathode to establish an RF discharge. Biasing of the PHV/NHV and varying the flowrate to the thruster, allowed a sensitivity mapping to be performed to establish some baseline operating points.

Following this set of 'baseline' characterization tests, the DN3.4 replaced the hollow cathode, and again a sensitivity map was established to allow ignition of the RF discharge. Although successful, the levels at which the PPU had to operate the PHV/NHV were not compliant to the development of the PPU and also schedule for the HENON mission, so a pressure shock start was baselined and this is the configuration shown in Fig 17. This series of coupling tests allowed optimization of the defined operating points for the HENON mission and also demonstrated that the DN3.4 was able to neutralize an ion beam up to 35.5mA (@2.5mN).

The RIT3.5 thruster has been shown to meet the required thrust range, power consumption, and specific impulse (Isp) through preliminary ground-mode testing. These tests were conducted by shorting the SSG to ground across the clamping network. In parallel with the RIT3.5 and DN3.4 developments, the flight Power Processing Unit (PPU), including the Radio Frequency Generator (RFG), was also under development. At the time of testing, the PPU was in an early breadboard configuration and was suitable only for operation in atmospheric conditions.

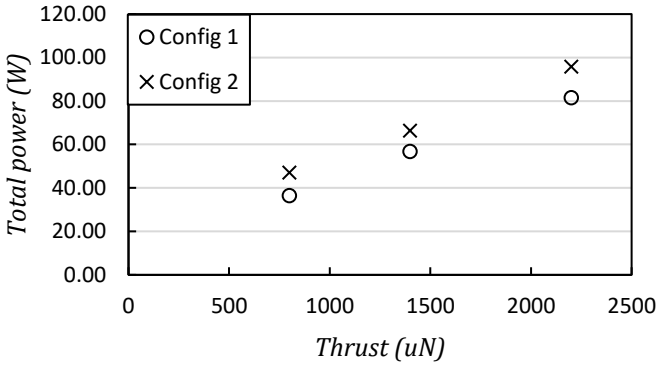

Figure 19. RIT3.5 grounded mode testing p total power (RFG + beam power) vs thrust with config 1: RFG in the vacuum chamber and config 2 RFG external to vacuum

A key difference introduced during testing with an external RFG was the extended harness length, necessitated by the RFG's location outside the vacuum chamber. It is well established that RFG power requirements are highly sensitive to cable length, as longer harnesses introduce higher transmission losses. To reduce uncertainty in early testing, an alternative laboratory-grade RFG capable of in-vacuum operation was used. The data presented in this section were collected under that configuration.

Initial commissioning tests were conducted to demonstrate stable operation across the target thrust range. The thruster was operated between 150 µN and 2.5 mN, exceeding mission requirements. As part of commissioning, a series of mass flow sweeps was performed to establish baseline operating conditions aligned with mission expectations. At three thrust setpoints (0.8, 1.4, and 2.2 mN), the mass flow rate was increased in 5% increments. RFG power was adjusted to return the system to the desired thrust setpoint, and data were recorded once electrical stability was achieved. The target beam current variation was less than 1% per hour for electrical stability. The same procedure was repeated with decreasing flow rates, starting from the initially predicted nominal values.

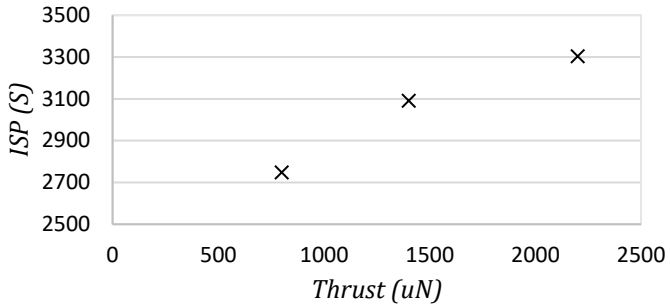

Figure 20. RIT3.5 grounded mode testing ISP vs thrust

This testing produced power versus mass flow relations for the three thrust levels. Based on these results, nominal flow rates of 0.302, 0.470, and 0.691 sccm were provisionally selected to enable follow-on testing. These values represent a trade-off between power and Isp, accounting for beginning-of-life performance and thus providing margin for system aging effects. The selected operating points will be re-evaluated during future endurance testing and with the flight-representative RFG.

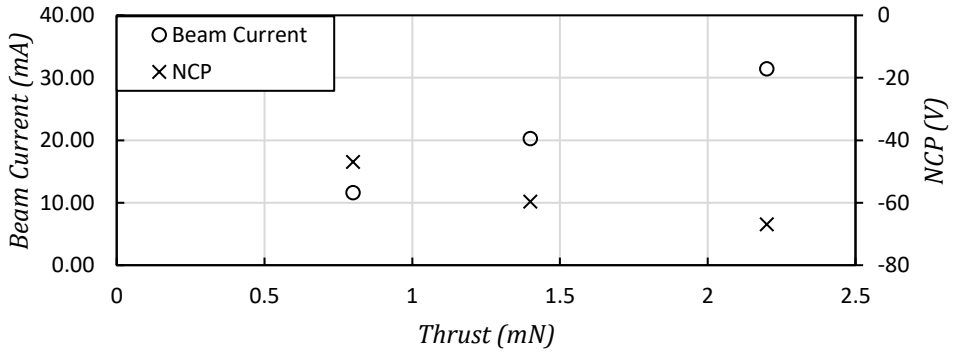

Figure 21: RIT3.5 & DN3.4 coupled mode operation, current neutralization and NCP from 0.8 to 2.2 mN operation for an 80 V casing and 400 V gate potential

The DN3.4 is capable of emitting sufficient current for neutralisation without being directly exposed to the beam potential. This is achieved through electrostatically enhanced emission, utilising focusing, gate, and casing electrode potentials to overcome the space-charge limitations of pure thermionic extraction. As a result, the dry cathode can be positioned externally to the beam, extending operational lifetime by reducing sputter erosion.

A series of system-level coupling tests were conducted using a BB Techline RFG together with an Argotec PCDU and a solar array simulator, enabling full end-to-end electrical de-risking and verification. Note, the BB Techline RFG was located external to the vacuum chamber. This resulted in the RFG power being highly sensitive to harness length, with increased cable length resulting in greater transmission losses. Consequently, the external RFG configuration, with its extended harness length, represents a conservative operating condition when interfaced with the PCDU, without compromising the validity of the configuration de-risking.

To provide reasonable estimates of the total operational power, an adjustment was required to account for the increased power demand resulting from the external RFG placement. Data from previous testing, conducted using an alternative ESA-provided in-vacuum capable RFG, included a comparison between in-vacuum and external RFG operation. These tests indicated an increase in RFG power consumption of approximately 50–70 percent when operating externally.

Based on this prior data, a simplified correction function was derived to estimate the corrected total RFG power:

$$P_{RFG,C} = P_{RFG}\eta$$

where P_{RFG} is the measured total RFG input power, and η is an empirical correction coefficient given by:

$$\eta = -1.79 \times 10^{-7}T^2 + 5.567 \times 10^{-4}T + 0.2493$$

This correction is valid over a thrust range, T, of 0.8–2.2 mN.

In addition, the Techline BB PPU incorporated an incorrectly sized resistor that caused the GaN FET to operate at elevated temperatures. Together with other suboptimal component selections in this BB model, the efficiency was reduced to approximately 70–75 percent during the integration test. Subsequent load-rack testing of the PPU with corrected components confirmed an efficiency of 87 percent, with further improvements in the EM variant expected to exceed 90 percent. As with the RFG harness, this inefficiency was treated as a conservative operating condition when interfaced with the PCDU for de-risking. For estimation of the PCDU total input power, however, an efficiency factor of 80.46% is applied to correct for the component efficiency.

As a result of these combined inefficiencies, the system current exceeded the LCL trip level when approaching 2.5 mN operation. The LCL trip occurred as expected for that current draw and successfully demonstrated the protective function, although it limited operation to the 2.2 mN upper set-point during these tests.

Figure 22 presents the estimated RIT3.5 and DN3.4 power, and Figure 23 shows the estimated total PCDU input power, both indicating compliance with margin relative to the 130 W CubeSat requirement. As expected, the thrust-to-power efficiency increased at higher thrust setpoints, while the ISP also improved, as shown in Figure 8. This demonstrates that operating at the highest thrust setpoint enhances overall system performance. The trend can be attributed to the RF plasma generation process, which requires relatively more energy per ion extracted at lower thrust setpoints. At higher beam currents, corresponding to higher thrust, the extraction grids operate closer to their design point, improving the ratio of thrust to RF input power. Furthermore, for the estimated PCDU input power, the semi-fixed power consumption overhead of the PCDU and PPU system was also accounted for, further enhancing efficiency at higher thrust levels.

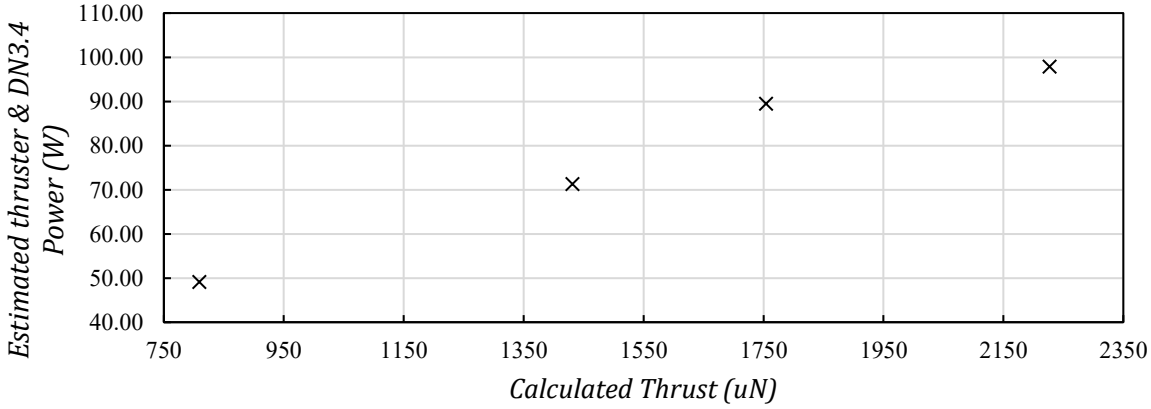

Figure 22: Total Thruster & DN Power, calculated as the sum of the high voltage supply powers (P-PHV + P-NHV) , RFG PSU power, and the heater power, gate supply power and casing supply power against calculated thrust from 800 µN to 2200 µN.

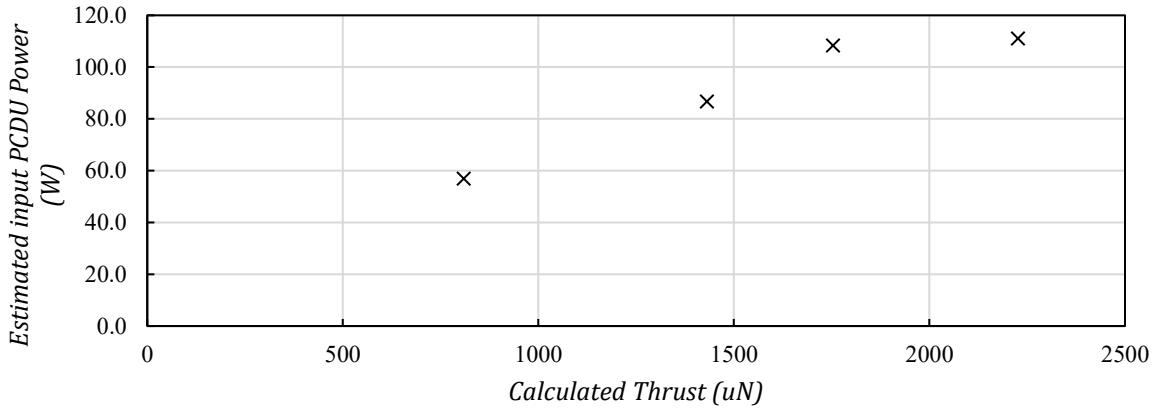

Figure 23: Argotec PCDU Power, given as provisional data from Argotec Personnel, against calculated thrust from 800 µN to 2200 µN.

Finally, Figure 24 illustrates the estimated PCDU input power across the full ignition cycle, from fully off to the maximum thrust setpoint. The sequence comprises transition from OFF to Standby, DN heater PSU activation, DN gate/casing PSU activation, RFG PSU activation, PHV/NHV activation, discharge mode operation, and subsequent thrust increase from 800 µN to 2200 µN. The RFG operation represents one of the largest power draws. During discharge ignition the RF impedance decreases, reducing power consumption relative to the pre-ignition standby state. Once in extraction mode, the PHV begins drawing current, leading to a higher power demand that scales with thrust. As with the previous plots, the system shows good alignment with requirements.

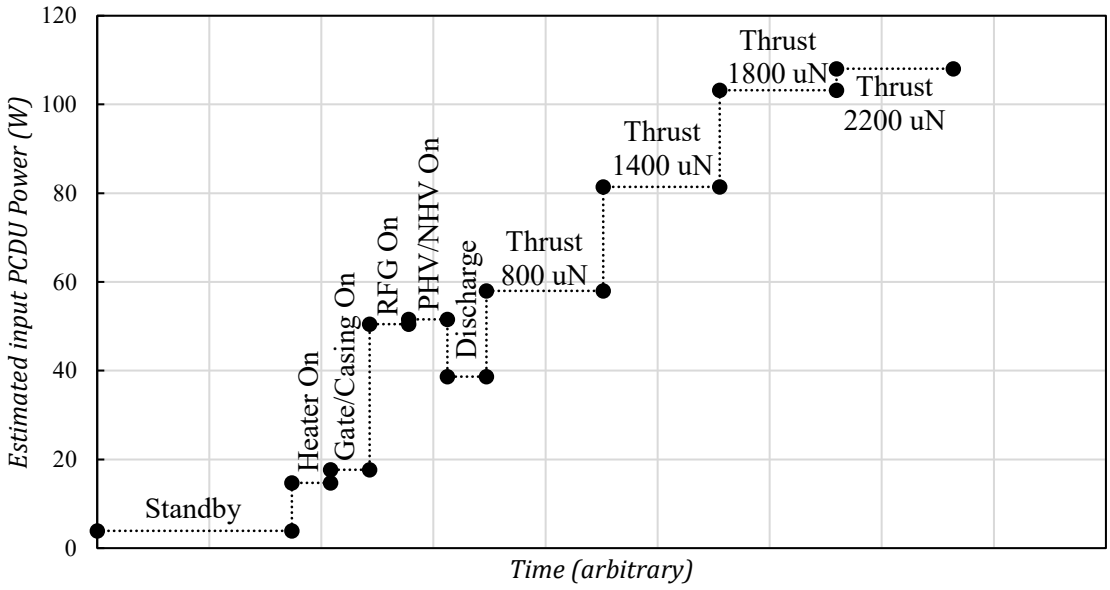

Figure 24: Power (DC) vs Time (arbitrary scale) of Argotec PCDU

XII. Cubesat AIT

A streamlined approach to the flight hardware has been developed for the HENON mission, mainly due to the aggressive launch window and associated platform level AIT procedure. Units will undergo a basic acceptance test campaign, excluding mechanical and thermal acceptance testing, before being available for integration into the EPROP module. Due to the layout of the small EPROP Module, a logical method of unit integration will be undertaken by MSL, initial steps including the assembly PFM EPROP frame being integrated to the S/C STM structure. The PSMS will undergo assembly and welding, including cleaning, leak testing and proof pressure testing. End-to-end functional tests of the main EPROP components (namely RIT3.5, DN3.4 and TPM/TPME) will then be performed, using representative EGSE where appropriate in place of the PPU's, to perform key interface compatibility testing.

The PPU's and associated harnessing are then finally integrated to the EPROP module, allowing the opportunity to perform bench level acceptance testing to ensure the associated power and interfacing to the module are functionally (limited to atmospheric testing only). The entire module (EPROP & S/C STM) undergo an acceptance firing campaign prior to the mechanical test campaigns, where the PCDU and OBC simulators are used to power and command the module. Due to the compact size of the entire stack, accommodation inside the vacuum chamber are foreseen.

Following this baseline acceptance campaign, the EPROP and S/C STM will undergo a full mechanical test campaign at qualification levels/acceptance durations in all 3-axis, with basic functional health checks performed between each axis. The full post performance tests will also form the start of the thermal acceptance test campaign where the EPROP and S/C STM will undergo four full cycles.

Following the test campaigns above, the EPROP module is removed from the S/C STM and will undergo final inspection/cleaning before being packed and sent for integration to the HENON spacecraft.

XIII.Conclusion

MSL, in conjunction with the agency, have developed a detailed set of requirements in which the CPS hardware have been under development. Advancements in manufacturing processes has given confidence to a compliant propellant tank design. Using mature, off-the-shelf hardware, such as the FMS and CGTs, the PSMS architecture is in an advanced state, with only the custom layout and interconnecting welds to address along with the thermal control aspect, in which MSL is undertaking as part of the system engineering role.

Preliminary coupling tests achieved operation beyond the HENON mission requirements, and as a de-risk, the CPS hardware performed above expectations. Further coupling tests are foreseen, along with the formal qualification of the sub-assemblies and optimisation of the AIT procedures to integrate the hardware into the compact volume.

MSL believe that the CPS architecture that has been developed will advance CubeSat operations beyond that of the current and will allow enhancement of future mission concepts.

Acknowledgments

Mars Space would like to acknowledge the continuing support from the European Space Agency, as well as the collaborations with TransMIT for the development of the RIT3.5 along with inputs from the Cubesat EPROP sub-contractors, namely; TWI (Propellant Tanks), Techline Systems Limited (PPU), Bradford Engineering (FMS), AVS (TPM/TPME) and Nammo (CGT).

References

[1]Guarducci, F., Lewis, R., Daykin-Iliopoulos, A., Marangone, D., and Clark, S., "Development and Industrialization of Miniature Radiofrequency Ion Thruster (RIT3.5) and Neutralizer Technologies for Precision Control Satellite Applications," The 38th International Electric Propulsion Conference, 2024

[2]Provinciali, L., et al., "HENON – Main Challenges of a Space Weather Alerts CubeSat Mission," 2024 IEEE Aerospace Conference, Big Sky, MT, USA, 2024, pp. 1-12, doi: 10.1109/AERO58975.2024.10521299.

[3]Guarducci, F., Marangone, D., Clark, S., Lewis, R., Gabriel, S.B., Smirnova, M., Mingo, A. "Development and Industrialization of the RIT3.5.", The 37th International Electric Propulsion Conference, Massachusetts Institute of Technology, USA, June 19-23, 2022

[4]Gasa, K., Rogers, E., Gabriel, S., Daykin-Iliopoulos, A., Bosi, F., and Guarducci, F. “Development of a Low Current Dry Neutralizer in a Pierce Gun Configuration.”, The 37th International Electric Propulsion Conference, Massachusetts Institute of Technology, USA, June 19-23, 2022

[5]Gasa, K., Gabriel, S., Nagadowska, Z., Guarducci, G., Daykin-Iliopoulos, A., "Experimental Characterization of a Low Current Dry Neutralizer", IEPC-2024-402, The 38th International Electric Propulsion Conference, Toulouse, France, June 23-28, 2024

[6]Gasa, K., Gabriel, S., Guarducci, G., Daykin-Iliopoulos, A., "Two-dimensional modelling of a low current electron gun dry neutralizer for ion engines", IEPC-2024-404, The 38th International Electric Propulsion Conference, Toulouse, France, June 23-28, 2024

[7]Robert-Jan Koopmans, Patrick van Put and Johan Kuiper, “Qualification status and prospects of the Low Power Fluid Management Systems”, IEPC-2025-686, The 39th International Electric Propulsion Conference, Imperial College London, London United Kingdom, 14-19 September 2025

[8]Alexander J.N. Daykin-Iliopoulos, Rhodri Lewis, Dominic Marangone, James Clover, Stephen Clark, Francesco Guarducci, Klevis Gasa, Stephen B. Gabriel, Maria Smirnova, Joseph Kigonya, Daniele Rizzieri, Davar Feili, Hassam Israel Guevara Jelid and Neil Wallace, “Radio Frequency Ion Engine and Dry Neutralizer Development and Coupled Testing for CubeSat Missions”, IEPC-2025-686, The 39th International Electric Propulsion Conference, Imperial College London, London United Kingdom, 14-19 September 2025

[9]Dominic Marangone, Francesco Guarducci, Stephen Clark, Rhodri Lewis, Andrea Fiaschi, Ugo Cesari, Maria Smirnova, Aloha Mingo, michele Coletti and Davar Feili, “Performance Characterization of the RIT3.5 Radiofrequency Ion Thruster coupled with the HC4 Hollow Cathode Neutralizer”, IEPC-2025-649, The 39th International Electric Propulsion Conference, Imperial College London, London United Kingdom, 14-19 September 2025

[10]Smirnova, M., Mingo, A., Schein, J., Smirnov, P., Bosch, E., Massotti, L., “Test Campaign on the novel Variable Isp Radio Frequency Mini Ion Engine.” The 36th International Electric Propulsion Conference, IEPC-2019-A-574, Vienna, Austria, September 15-20, 2019